The 12th International Conference of
International Association for Computer Methods and Advances in Geomechanics (IACMAG)
1-6 October, 2008
Goa, India

TIME DEPENDENT DEFORMATIONS IN SQUEEZING TUNNELS

G. Barla, M. Bonini and D. Debernardi
Department of Structural and Geotechnical Engineering, Politecnico di Torino, Italy

Keywords: tunnelling, squeezing, time dependent behaviour, numerical modelling

ABSTRACT: This paper deals with full face excavation of large size tunnels in rock masses of very poor quality which exhibit squeezing behaviour. Time dependence is accounted for explicitly by using constitutive models which have been validated with reference to laboratory testing and in situ performance monitoring. The case study of the Saint Martin La Porte access adit (Lyon-Turin Base Tunnel) is taken as illustration. In this adit an innovative excavation-construction method is being used to cope with the severely squeezing Carboniferous zone encountered. An essential feature of this method is a two-stage excavation sequence with installation of a composite pre-reinforcement/reinforcement system with deformable elements embedded in the shotcrete lining. The tunnel response has been analysed by both semi-analytical and numerical solutions with close attention paid to the constitutive models adopted. Results of modelling are compared with convergence monitoring data.

1 Introduction

Tunnel construction in squeezing conditions is very demanding due to the difficulty in making reliable predictions at the design stage. During excavation such conditions are not easily anticipated, even when driving into a specific geological formation and experience is gained on the squeezing problems encountered. Squeezing conditions may vary over short distances due to rock heterogeneity and fluctuations in the mechanical and hydraulic properties of the rock mass. Indeed, the selection of the most appropriate excavation-construction method (i.e. mechanized tunnelling versus conventional tunnelling) is highly problematic and uncertain. Due to the fixed geometry and the limited flexibility of the TBM (Tunnel Boring Machine) allowable space to accommodate ground deformations is restricted. On the contrary, in conventional tunnelling a considerably larger profile can be excavated initially in order to allow for large deformations. The obvious consequence is that in deep tunnels, whenever severely squeezing conditions are anticipated, conventional tunnelling appears to be preferred over mechanized tunnelling.

Squeezing is essentially a time dependent behaviour although for design purposes the rock mass which undergoes squeezing is often represented as an equivalent elastic-plastic medium with strength and deformability parameters which are down-graded based on observation and monitoring during excavation. The so called "short term" and "long term" conditions are often invoked, characterized by different values of the parameters involved in the constitutive model being used. However, there is no doubt that under the most severe squeezing conditions an appropriate representation of the tunnel response is obtained only by using constitutive models which account for time dependent behaviour. This originates from the fact that time dependent deformations are observed whenever face advancement is stopped and these are likely to take place during excavation, when it is difficult to distinguish the "face effect" from the "time effect".

This paper deals with full face excavation of large size tunnels in rock masses which exhibit squeezing behaviour. This is considered explicitly by using three constitutive models which have been validated during the years following the 11th IACMAG Conference in Torino (Barla, 2005). The case study of the Saint Martin La Porte access adit along the Lyon-Turin Base Tunnel is taken as illustration.

2 Squeezing behaviour

The term "squeezing" originates from the pioneering days of tunnelling through the Alps. It refers to the reduction of the tunnel cross section that occurs as the tunnel is being advanced (Figure 1). Based on the work of a Commission of the International Society for Rock Mechanics (ISRM), which has described squeezing and the main features of this mechanism, it is agreed that "squeezing of rock" stands for large time dependent convergence during tunnel excavation. This happens when a particular combination of material properties and induced stresses causes yielding in some zones around the tunnel, exceeding the limiting shear stress at which creep starts. Deformation may terminate during construction or continue over a long period of time.

The magnitude of tunnel convergence, the rate of deformation, and the extent of the yielding zone around the tunnel depend on the geological and geotechnical conditions, the in situ state of stress relative to rock mass strength, the groundwater flow and pore water pressure, and the rock mass properties. Squeezing is therefore synonymous with yielding and time-dependence, and often is largely dependent on the excavation and support techniques being used. If the support installation is delayed, the rock mass moves into the tunnel and a stress redistribution takes place around it. On the contrary, if deformation is restrained, squeezing will lead to long-term load build-up of the support system.

Figure 1. Squeezing rock reduces the tunnel cross section. This is shown in this photograph where re-profiling of a highly deformed cross section is taking place in the Saint Martin access adit (Lyon-Turin Base Tunnel).

3 Time-dependent constitutive models

In order to describe the tunnel response associated with severely squeezing conditions, time dependent constitutive models need be used. In the following a viscoelastic-plastic model (CVISC), an elastic-viscoplastic model (VIPLA) and a more complex elastic-plastic-viscoplastic model (SHELVIP) are briefly described.

3.1 CVISC model

The CVISC model (Itasca, 2006) is an analogical model which couples, in series, the Burgers viscoelastic model (i.e. Kelvin and Maxwell models in series) with a plastic flow rule, based on the Mohr-Coulomb yield criterion, as shown in Figure 2.

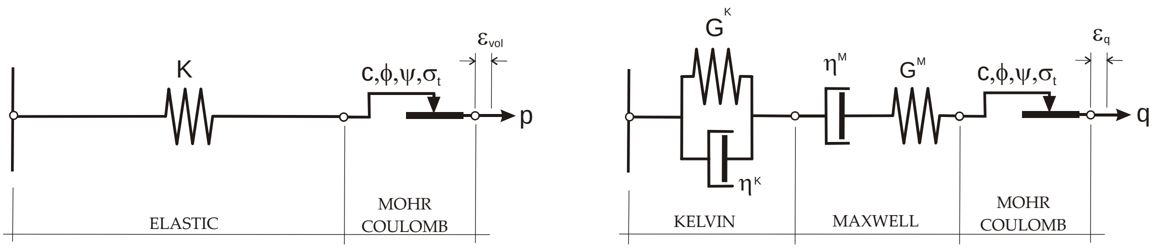

(a) Volumetric behaviour (b) Deviatoric behaviour

Figure 2. Sketch of the CVISC model: (a) volumetric behaviour, and (b) deviatoric behaviour.

The volumetric behaviour is only elastic-plastic and is governed by the linear elastic law and the plastic flow rule (Figure 2.a), while the deviatoric behaviour is viscoelastic-plastic and is driven by the Burgers model and the same plastic flow rule (Figure 2.b). This means that the viscoelastic strains are deviatoric and depend only on the deviatoric stress state; instead the plastic strains are both deviatoric and volumetric and depend on the global stress in accordance with the chosen flow rule.

3.2 VIPLA model

The VIPLA model (Lemaitre & Chaboche, 1996) is based on Perzyna's overstress theory (Perzyna, 1966) which states that the strain rate tensor $\dot{\varepsilon}_{ij}$ can be split into elastic $\dot{\varepsilon}_{ij}^{e}$ and viscoplastic $\dot{\varepsilon}_{ij}^{vp}$ components, to give:

$$\dot{\varepsilon}_{ij} = \dot{\varepsilon}_{ij}^{e} + \dot{\varepsilon}_{ij}^{vp} \tag{1}$$

The viscoplastic strain rate tensor $\dot{\varepsilon}_{ij}^{vp}$ can be calculated by the following flow rule:

$$\dot{\varepsilon}_{ij}^{vp} = \gamma \cdot \Phi\left(\langle F \rangle\right) \cdot \frac{\partial g}{\partial \sigma_{ij}} \tag{2}$$

where γ is the fluidity parameter, F is the over-stress function, representing the distance from the yield surface $f = 0$, $\Phi(F)$ is the so-called viscous nucleus, g is the viscoplastic potential and σ_{ij} the stress tensor.
The time-dependency is introduced in this model by modifying the classical flow rule of elastoplasticity and by discarding the consistency rule $(df = 0, f \le 0)$, thus allowing the yield function f to be positive or negative. The viscoplastic potential g defines the direction of $\dot{\varepsilon}_{ij}^{vp}$, while F influences its modulus by means of the viscous nucleus Φ.
In the VIPLA model F is assumed to be represented by the yield function f and Φ is assumed to be a power law:

$$\Phi = \langle F \rangle^{n} = \langle f \rangle^{n} \tag{3}$$

where n is a constitutive parameter $(n \ge 1)$.
The yield function f is splitted into a part $\bar{f}$, which depends only on the stress state, and a part κ, which depends only on the viscoplastic strain, according to:

$$f = \frac{\bar{f}\left(\sigma_{ij}\right)}{\kappa\left(\varepsilon_{ij}^{vp}\right)} \tag{4}$$

For the function $\bar{f}$ the Von Mises yield criterion is assumed:

$$\bar{f}\left(\sigma_{ij}\right) = q \tag{5}$$

where q is the stress deviator.
A potential hardening is introduced by means of the function κ:

$$\kappa\left(\varepsilon_{ij}^{vp}\right) = \left(\varepsilon_{q}^{vp}\right)^{-m/n} \tag{6}$$

where m is a constitutive parameter $(1 - n < m \le 0)$ and ε_{q}^{vp} is the deviatoric viscoplastic strain, $\varepsilon_{q}^{vp} = \sqrt{4/3 \cdot J_{2,\varepsilon^{vp}}}$ where $J_{2,\varepsilon^{vp}}$ is the second invariant of the viscoplastic strain deviator.
Under these assumptions, the yield surface $f = 0$ is reduced to the hydrostatic axis and it does not change with time.
The viscoplastic potential g is taken to be equal to $\bar{f}$ (i.e. the flow rule is associated). With these assumptions, the viscoplastic strains depend only on the deviatoric stress state and do not induce volumetric strains. Therefore, Eqn. (2) becomes:

$$\dot{\varepsilon}_{ij}^{vp} = \frac{3}{2} \cdot \gamma \cdot q^{n-1} \cdot \left(\varepsilon_{q}^{vp}\right)^{m} \cdot s_{ij} \tag{7}$$

The constitutive parameters n and m define respectively the dependence of the viscoplastic strain rate tensor on the deviatoric stress and on the equivalent viscoplastic strain, whereas the parameter γ defines the amplitude of the viscoplastic strains.

3.3 SHELVIP model

The SHELVIP model (Stress Hardening ELastic VIscous Plastic model) is derived from the Perzyna's overstress theory, by adding a time independent plastic component (Debernardi, 2008). Therefore it is possible to split the strain rate tensor $\dot{\varepsilon}_{ij}$ into elastic $\dot{\varepsilon}_{ij}^{e}$, plastic $\dot{\varepsilon}_{ij}^{p}$, and viscoplastic $\dot{\varepsilon}_{ij}^{vp}$ components, to give:

$$\dot{\varepsilon}_{ij} = \dot{\varepsilon}_{ij}^{e} + \dot{\varepsilon}_{ij}^{p} + \dot{\varepsilon}_{ij}^{vp} \tag{8}$$

According to the classical theory of elastoplasticity, the time-independent plastic strains ε_{ij}^{p} develop only when the stress point reaches the plastic yield surface $f_p = 0$ (Figure 3), defined by the Drucker-Prager criterion:

$$f_p = q - \alpha_p \cdot p - k_p \tag{9}$$

The plastic strains ε_{ij}^{p} can be evaluated using the classical flow rule of elastoplasticity:

$$\varepsilon_{ij}^{p} = \lambda \cdot \frac{\partial g_p}{\partial \sigma_{ij}} \tag{10}$$

where g_p is the plastic potential, $g_p = q - \omega_p \cdot p$, that defines the direction of ε_{ij}^{p}, ω_p is the plastic dilatancy and λ is the plastic multiplier, that can be determined using the consistency condition $df_p = 0, f_p \le 0$.

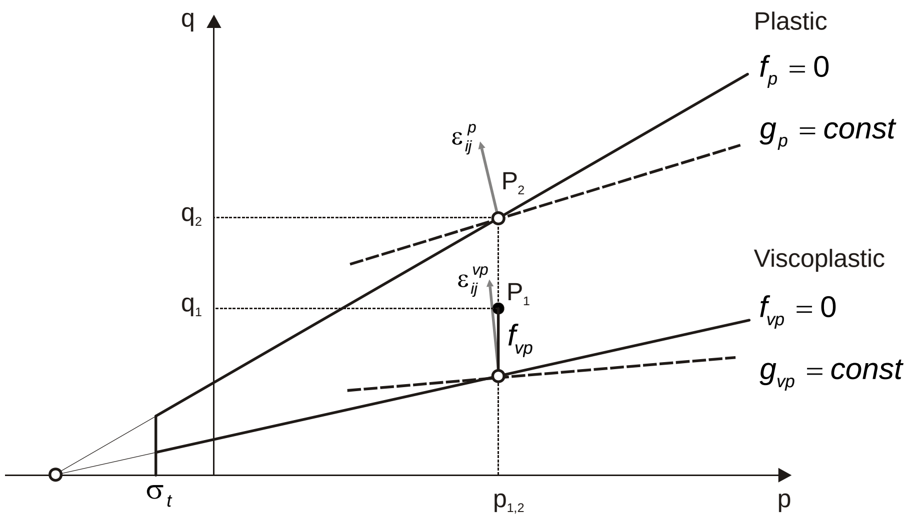

Figure 3. Schematization of the SHELVIP model in the p-q plane.

The viscoplastic strain rates $\dot{\varepsilon}_{ij}^{vp}$ develop only if the effective stress state exceeds a viscoplastic yield surface $f_{vp} = 0$ (Figure 3) which is also defined by the Drucker-Prager criterion. This surface is internal to the plastic yield surface and intersects the p-axis at the same point as the plastic yield surface. Thus, it is possible to write:

$$f_{vp} = q - \alpha_{vp} \cdot \left(p + \frac{k_p}{\alpha_p} \right) \tag{11}$$

where α_{vp} is a visco-hardening parameter that defines the internal viscous state of the material.
The viscoplastic $\dot{\varepsilon}_{ij}^{vp}$ strain rate can be determined using the flow rule of Perzyna's overstress theory:

$$\dot{\varepsilon}_{ij}^{vp} = \gamma \cdot \Phi\left(\langle F \rangle\right) \cdot \frac{\partial g_{vp}}{\partial \sigma_{ij}} \tag{12}$$

The overstress function F is assumed to be equal to the viscoplastic yield function f_{vp} and the viscous nucleus Φ to be a power law:

$$\Phi = \langle F \rangle^n = \langle f_{vp} \rangle^n \tag{13}$$

where n is a constitutive parameter.
The viscoplastic potential g_{vp} is assumed to be $g_{vp} = q - \omega_{vp} \cdot p$, where ω_{vp} is the viscoplastic dilatancy.
The hardening of the viscoplastic yield surface is governed by the differential equation:

$$\dot{\alpha}_{vp} = \frac{l}{m \cdot n} \cdot \frac{f_{vp}}{p + k_p / \alpha_p} \cdot \left(\frac{f_{vp}}{q} \right)^{n \cdot m} \tag{14}$$

where m and l are constitutive parameters.

4 The Saint Martin La Porte access adit

The CVISC, VIPLA, and SHELVIP constitutive models have been used to back analyse the tunnel response based on convergence monitoring in representative sections of the Saint Martin La Porte access adit. An illustration of the geological conditions and of the excavation-support system adopted in this tunnel is given below.

4.1 Geological conditions and excavation-support systems

The Saint Martin La Porte access adit (Figures 4.a and 4.b) is being excavated in the Carboniferous Formation, “Zone Houillère Briançonnaise-Unité des Encombres“ (hSG in Figure 4.a), which is composed of black schists (45 to 55%), sandstones (40 to 50%), coal (5%), clay-like shales and cataclastic rocks. A characteristic feature of the ground observed at the face during excavation (Figure 4.b) is the highly heterogeneous, disrupted and fractured conditions of the rock mass which exhibits very severe squeezing problems. The formation is affected often by faulting that results in a degradation of the rock mass conditions. The overburden along the tunnel in the zone of interest ranges from 300 m to 550 m. Excavation takes place in essentially dry conditions.
In order to assess the rock mass quality during excavation, detailed mapping of the geological conditions at the face was undertaken as depicted in Figure 4.b. This provides information to evaluate the percent distribution of “strong” (sandstones and schists) and “weak” (coal and clay-like shales) rocks at the face.

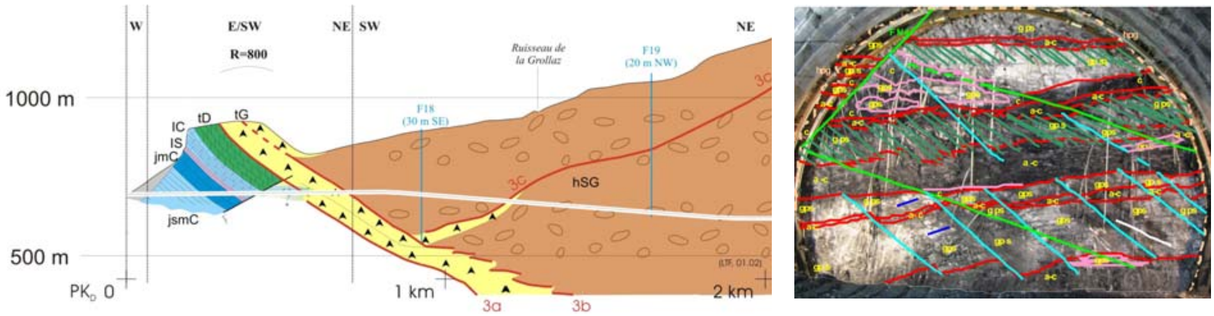

(a) (b)

Figure 4. (a) Geological profile along the Saint Martin La Porte access adit and (b) typical geological conditions at the face at chainage 1480 m (gps-sandstones, a-clay like shales, c-coal, etc.).

Several support systems were used in the Carboniferous zone. However, it soon became apparent that a stiff support would not be feasible in the severely squeezing conditions encountered. The design concept finally chosen (Figure 5.b) was based on allowing the support to yield while using full-face excavation with systematic face reinforcement by fiber-glass dowels. The support system initially implemented (Figure 5.a) consisted of yielding steel ribs with sliding joints (TH, Toussaint-Heintzmann type), rock anchors and a thin shotcrete layer in a horseshoe profile. These sections of the tunnel underwent very large deformations with convergences up to 2 m and later needed to be re-profiled.

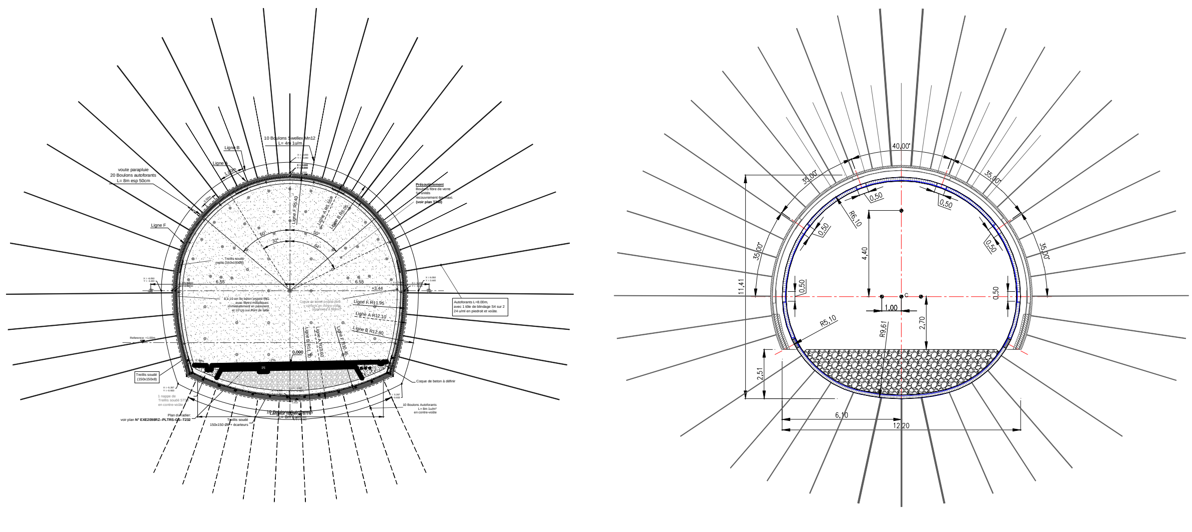

(a) (b)

Figure 5. Tunnel cross section showing the excavation-support systems adopted in the Saint Martin La Porte access adit between chainage 1267 and 1324 m (P7.3, a) and chainage 1325 and 1700 m (DSM, b).

In order to improve the working conditions and to control deformations, a novel support system was implemented with a near circular cross section. This can be summarized as follows (Figure 5.b):

- Stage 0: face pre-reinforcement, including a ring of grouted fiber-glass dowels around the opening, designed to reinforce the rock mass ahead and around the tunnel perimeter over a 2 to 3 m thickness.
- Stage 1: mechanical excavation carried out in steps of one meter length, with installation of a support system consisting of untensioned rock anchors (length 8 m) along the perimeter, yielding steel ribs with sliding joints (TH type), and a 10 cm thick shotcrete layer. The tunnel is opened in the upper cross section to allow for a maximum convergence of 600 mm.
- Stage 2: the tunnel is opened to the full circular section at a distance of 15-25 m from the face, with application of 20 cm shotcrete lining, yielding steel ribs with sliding joints (TH type) with 9 longitudinal slots (one in the invert) fitted with HiDCon (High Deformable Concrete) elements. The tunnel is allowed to deform in a controlled manner to develop a maximum convergence which should not exceed 400 mm.
- Stage 3: installation of a coffered concrete ring at a distance of 80 m from the face.

4.2 Controlled response of the tunnel deformation

Systematic monitoring of tunnel convergence is underway along the tunnel. Convergences are measured by means of optical targets placed along the tunnel perimeter. A number of special sections have been equipped with multi-position borehole extensometers and strain meters located across the HiDCon elements. Extrusometer monitoring has been used to measure the longitudinal displacement ahead of the tunnel face. In addition, the strain level in the primary lining has been monitored (Barla et al., 2007).

In order to gain in the understanding of the tunnel response so far, it is of interest to consider Figure 6.a, which shows the tunnel "deformation" that has occurred (i.e. the convergence divided by the length of each array measured at the time of installation of the optical targets) in stage 1 along arrays 1-3, 3-5 and 1-5 (Δl_{i-j}) between chainage 1200 m and 1700 m, with the tunnel face being 15 m ahead of the monitoring section. Also illustrated in Figure 6.b are the convergences occurred along array 1-5 in stage 2 after 30, 80 and 120 days from the stage 2 installation. Three stops of face advance, represented in the figures by the vertical lines, took place along the tunnel length with the DSM cross section implemented.

The following observations can be made:

- Large deformations are associated with cross section P7.3 between chainages 1200 and 1400 m; with cross section DSM the convergences in stage 1 generally are smaller with the tunnel strain never in excess of 6-7 %.
- The 600-mm allowed convergence with cross section DSM has been exceeded locally (e.g., at chainage 1478 m due to the stop at chainage 1494 m and between chainages 1525 and 1550 m where the rock mass quality was very poor) and required re-profiling of the tunnel cross section before installing the composite lining adopted in stage 2.
- The tunnel deformation associated with cross section P7.3 appears to be rather different in one section with respect to the neighbouring one, which is not the case for cross section DSM.
- With chainage 1550 m approximately the tunnel response appears to exhibit smaller convergences in line with the improved rock mass conditions encountered, which appear even more encouraging around chainage 1700 m.

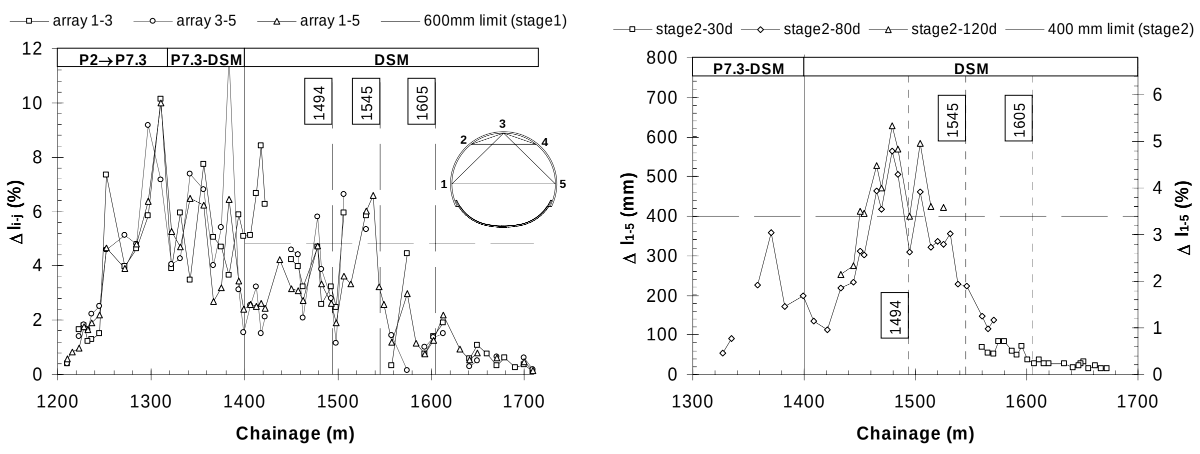

(a) (b)

Figure 6. (a) Deformations measured along arrays 1-3, 3-5 and 1-5 at 15 m from face in phase 1 and (b) convergences at 30, 80 and 120 days following excavation with stage 2 installed.

It also is important to consider the tunnel convergence versus time in stage 2 as depicted in Figure 6.b along array 1-5. This occurs at a significant distance from the advancing face and when the yielding support has been active for a certain time and the final concrete lining has not yet been installed. It is noted that between chainages 1450 and 1525 m the tunnel cross section experienced deformations in excess of that allowed (400 mm). In such a case the HiDCon elements on the right wall (looking at the tunnel face) attained 40% limit strain and visible overstressing occurred in them. This did not cause any significant problem as no difficulties were encountered before installing the final lining.

A back analysis of the monitored convergence data between chainages 1394 and 1507 m has been performed, using the following time-dependent relationship (Sulem et al., 1987):

$$C(x,t) = C_{\infty,x} \cdot \left[1 - \left(\frac{X}{x+X}\right)^2\right] \cdot \left\{1 + m \cdot \left[1 - \left(\frac{T}{t+T}\right)^{0.3}\right]\right\} \tag{15}$$

where $C(x,t)$ is the convergence at the distance x from the tunnel face and at the time t, $C_{\infty,x}$ is the convergence at distance x obtained in the case of an infinite rate of face advance (no time dependent effect), m is a non dimensional parameter which depends on the ground conditions, X is a distance related to the distance of influence of the face (for an elastic plastic model of behaviour $X = 0.84 \cdot R_{pl}$, with R_{pl} taken as the plastic radius of the tunnel), T is a characteristic parameter of the rock mass time dependent properties.

The results obtained are reported in Table 1. It is noted that the distance of influence of the face (this length may be estimated to be four times the value of X, Sulem et al., 1987) is considerable; also, the time dependent properties of the rock mass, which are related to the T parameter, are representative of the severity of the squeezing conditions encountered. The variability of parameters found out for $C_{\infty,x}$ and X are due to the different stiffness of the support installed more than a substantial change of geomechanical conditions of the rock mass. Moreover the similarity of time related parameters (T and m) signifies that the time-dependency is comparable.

Table 1. Representative parameters for the Saint Martin La Porte tunnel.

	$C_{\infty x}$ [mm]	X [m]	T [days]	m [-]
P7.3 profile* (1272-1322 m)	1563.1	81.1	25.0	1.29
DSM profile - phase 1* (1394-1507 m)	602.6	41.2	35.3	1.09

* the parameters have been evaluated according to the monitoring data between the chainages shown.

5 Modelling the tunnel response

The three constitutive models (CIVISC, VIPLA, and SHELVIP) described above have been adopted in order to analyse the tunnel response in terms of convergence monitored during excavation. As an illustration of the application of the VIPLA model the semi-analytical solution due to Nguyen-Minh and Pouya (1992) is discussed first. Then, numerical modelling by the Finite Difference Method and the FLAC code is applied in conjunction with the CIVISC and the SHELVIP constitutive models respectively. It is underlined that the purpose here is to see how three different constitutive models with different levels of complexity reproduce the time dependent deformations of the tunnel in different cross sections. It is implied that the experience gained is essential in order to be able to predict the tunnel behaviour with the expected higher overburden to be encountered as the excavation proceeds. The information provided is of relevance if one is to optimize the type of support adopted and the excavation/support sequence.

The numerical analyses presented are for two different cross sections, namely at chainage 1311 m and 1406 m, where the P7.3 and DSM support type were installed. One may question why so distant sections characterised by different support types were taken for testing respectively the CIVISC and the SHELVIP constitutive models. It is noted that for P7.3 the influence of the preliminary lining stiffness is negligible, so that axisymmetric modelling with total stress release on the tunnel boundary can be favourably implemented and interpreted. On the other hand, the study of the DSM cross section calls for an accurate representation of geometry, construction stages and properties of the structural elements adopted, which may be better achieved by modelling the problem in plane strain conditions.

5.1 Semi-analytical solution for the P7.3 cross section (VIPLA model)

A simple time dependent analysis of a tunnel which applies the VIPLA model can be obtained with the solution proposed by Nguyen-Minh and Pouya (1992). The main assumptions of this solution are as follows: (a) the tunnel is of circular section, is not lined and is sufficiently deep; (b) the problem can be treated in plane strain conditions; (c) the initial stress state is isotropic and homogeneous; the ground is homogeneous, isotropic, and incompressible (ν=0.5). Under these assumptions the radial viscoplastic strain rate $\dot{\varepsilon}_r^{vp}$ at the distance r from the tunnel centre at time *t* is given by the following expression:

$$\frac{\partial}{\partial\tau}\left(\frac{\varepsilon_r^{vp}}{\varepsilon_R^e}\right)^{\frac{1}{\alpha}}=\left\{u\left[1+(\beta-1)u^{\beta-1}\tau^{\alpha}\right]^{\frac{1}{1-\beta}}+u^{\frac{1}{\beta}}\frac{1}{\beta}\left\{1-\left[1+(\beta-1)u^{\frac{\beta-1}{\beta}}\tau^{\alpha}\right]^{\frac{1}{1-\beta}}\right\}\right\}^{\frac{\beta}{\alpha}} \tag{16}$$

$$\alpha=\frac{1}{1-m};\ \beta=\frac{n}{1-m};\ a=\left(\frac{\gamma}{\alpha}\right)^{\alpha};\ \tau=t\Bigg/\left(\frac{\varepsilon_R^e}{a_{cyl}\left(2\sigma_0\right)^{\beta}}\right)^{\frac{1}{\alpha}};\ \varepsilon_R^e=\frac{3}{2}\frac{\sigma_0}{E};\ a_{cyl}=a\left(\frac{\sqrt{3}}{2}\right)^{\beta+1};\ u=\left(\frac{R}{r}\right)^{2} \tag{17}$$

where R is the tunnel radius, σ_0 the isotropic stress state, ε_R^e the elastic radial strain at tunnel contour, E the elastic modulus, γ, m and n the constitutive parameters of the VIPLA model. With a double numerical integration, over time and over the tunnel radius, it is possible to obtain the tunnel radial displacement.
In order to account for the influence of the face on the tunnel radial displacement, the isotropic stress state need be reduced according to (Panet, 1995):

$$\frac{\bar{\sigma}_0}{\sigma_0}=0.28+0.72\left(1-\frac{0.84}{0.84+x/R}\right) \tag{18}$$

where x is the distance from the face and $\bar{\sigma}_0$ the reduced isotropic stress state which accounts for the face influence.
By fitting with the least square algorithm the radial displacements computed from the monitored tunnel convergences at chainage 1311 m the constitutive parameters of the VIPLA model are obtained as shown in Table 2. Figure 7 shows the comparison between the computed and the monitored radial displacements.

Table 2. Constitutive parameters of the VIPLA model (time in year and pressure in kPa)

E	1180 MPa
γ	2.25E-25
m	-1.32
n	6.16

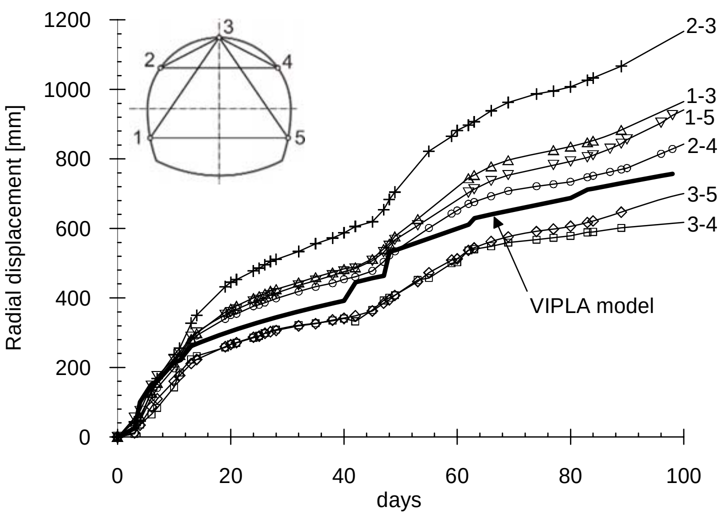

Figure 7. Computed (mean value) versus monitored radial displacements at chainage 1311 m.

5.2 Numerical modelling of the DSM cross section (CVISC model)

For the purpose of numerical modelling with the CVISC model the DSM cross section at chainage 1406 m has been chosen. The overburden is 400 m and the initial stress state is assumed to be isotropic and equal to 10 MPa. The analyses were performed with the Finite Difference Method and the FLAC code (Itasca, 2006). Figure 8.a shows the finite difference grid adopted in close proximity to the tunnel. The grid is made of square elements which increase in size away from the tunnel in order to minimize error propagation and solution time. Symmetry is assumed and half the tunnel section is modelled in plane strain conditions. The constitutive parameters for the CVISC model and the lining in stage 2 are shown in Table 3.
The model is to allow for simulation of the excavation/construction sequence in two stages. Overall five simulation steps have been implemented in order to represent this as accurately as possible. Following simulation of the initial stress state, the excavation of the top heading is performed with a stress release equal to 88% of the initial stress sate. The presence of the rock dowels around the tunnel and of the primary lining is simulated with a 200 kPa uniform pressure applied on the same tunnel boundary. The ground is initially taken as elastic perfectly

plastic and the time dependent behaviour during stage 1 is simulated by running the CVISC model for 23 days with the intent to match the tunnel response as observed through monitoring.

Following the invert excavation, where the rock mass behaviour is elastic perfectly plastic, the composite deformable lining is placed in the model, the applied pressure on the tunnel boundary is removed and the stress reduction process is completed. The composite deformable lining is modelled by beam elements, with a deformation modulus equal to 30000 MPa and a Poisson's ratio equal to 0.2. The presence of the HiDCon elements incorporated in the lining is simulated by beam elements with a linearly elastic ideally plastic behaviour and the mechanical properties listed in Table 3, where the mechanical parameters of the rock mass are also given.

An interface is introduced between the lining and the rock surround with normal (k_n) and shear (k_s) stiffness equal to $3.45 \cdot 10^3$ MPa/m and $3.45 \cdot 10^2$ MPa/m respectively. The analysis of stage 2 is obtained by running the CVISC model for 77 days with the intent to reproduce the observed tunnel response versus time with the convergence curve shown in Figure 8.b taken as target.

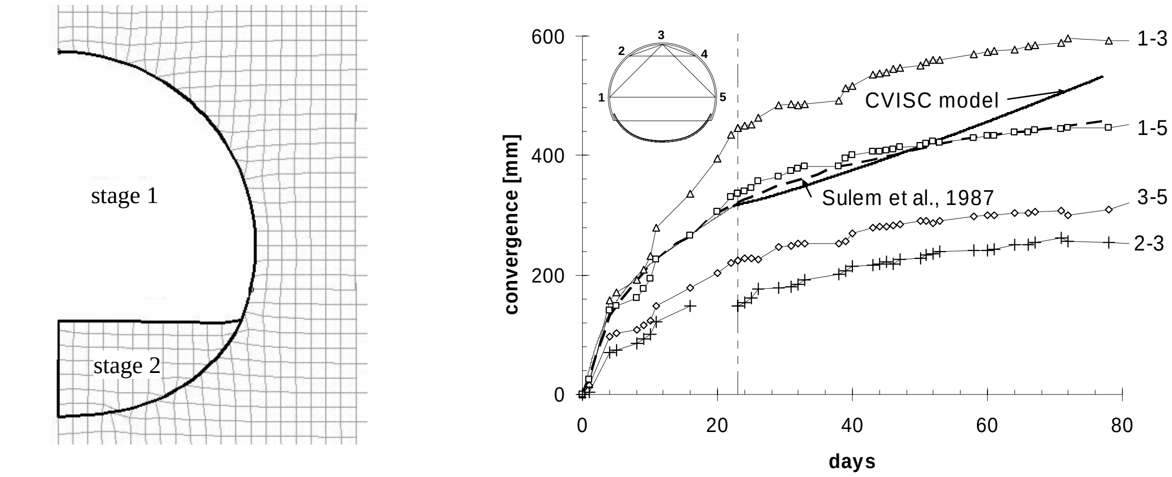

(a) (b)

Figure 8. (a) Cross section of Saint Martin La Porte tunnel in the numerical model.
(b) Computed (CVISC model) versus monitored convergence at chainage 1406 m.
Also shown is the convergence curve according to Sulem et al., 1987.

Table 3. Constitutive parameters for CVISC model and lining in stage 2.

Ground (CVISC model)	Units	Value
Deformation modulus, E	MPa	1441
Poisson's ratio, ν	-	0.25
Cohesion, c	MPa	0.61
Friction angle, φ	°	28
Kelvin viscosity, η_K	MPa·year	4.26
Kelvin shear modulus, G_K	MPa	498.1
Maxwell viscosity, η_M	MPa·year	27.98

Lining in stage 2	Units	Value
Thickness	m	0.2
Moment of inertia, I	m^4	$6.67 \cdot 10^{-4}$
Yielding stress, σ_y	MPa	8.5
Tensile strength, σ_t	MPa	0.85
Deformation modulus, E	MPa	5000
Poisson's ratio, ν	-	0.2

Figure 8.b shows the computed convergence plot versus time obtained for the cross section of interest and for a total duration of 80 days. Also shown in the same figure is the plot of the interpolation function (15) computed with the following characteristic parameters: T = 34.2 days, X = 23.7 m and m = 1.36.

It is shown that when the model simulates the tunnel "short term" response, the convergence along array 1-5, namely 314 mm, is very similar to the in situ value (336 mm) and to the interpretation according to Sulem et al. 1987 (320 mm). The tunnel convergence of stage 1 computed when the CVISC model is activated, reproduces quite well that observed in situ. It can be seen from Figure 8.b that the convergence versus time plot finally obtained with the numerical analyses compares well with the observed response up to 50 days duration time. As expected, the model does not predict the observed deformation thereafter, when the tunnel is shown to exhibit a gradual decrease in the rate of convergence, reaching a near stable condition.

5.3 Numerical modelling of the P7.3 cross section (SHELVIP model)

Particular attention has been paid to the numerical analysis of sections that have been excavated with the P7.3 support system, because they underwent very large deformations, with convergences up to 2 m. For this reason the novel SHELVIP model, that has been formulated particularly for numerical analysis of tunnel under severely squeezing conditions, has been adopted. The constitutive parameters obtained by fitting the results of creep and relaxation tests has been used as starting parameters for the back-analysis carried out.
The numerical analyses of the tunnel response were performed by the FDM and the FLAC code (Itasca, 2006) with the new SHELVIP model implemented (Debernardi, 2008). Axisymmetric conditions have been adopted in order to reproduce the three-dimensional influence of the tunnel face, which is known to play a significant role in squeezing conditions.
The tunnel cross section is assumed to be circular, with an equivalent radius of 5.5 m. Figure 9.a shows the FDM mesh adopted. The mesh is composed of perfectly square elements, with size increasing gradually from 0.5 m to 4 m when moving from the near vicinity of the tunnel outwards, in order to minimize error propagation and solution time. The total size of the mesh (184 m - 92 m) is very large in order to minimize the boundary effects that are very significant in the case of large deformations. The influence of the primary lining and the reinforcement system has been neglected.
As shown in Figure 9.b, particular attention has been posed on the chronological sequence of excavation (face advancement) which is considered to influence the time-dependent deformational response. The complex excavation sequence requires 245 computational steps, in order to closely follow the real chronological sequence.

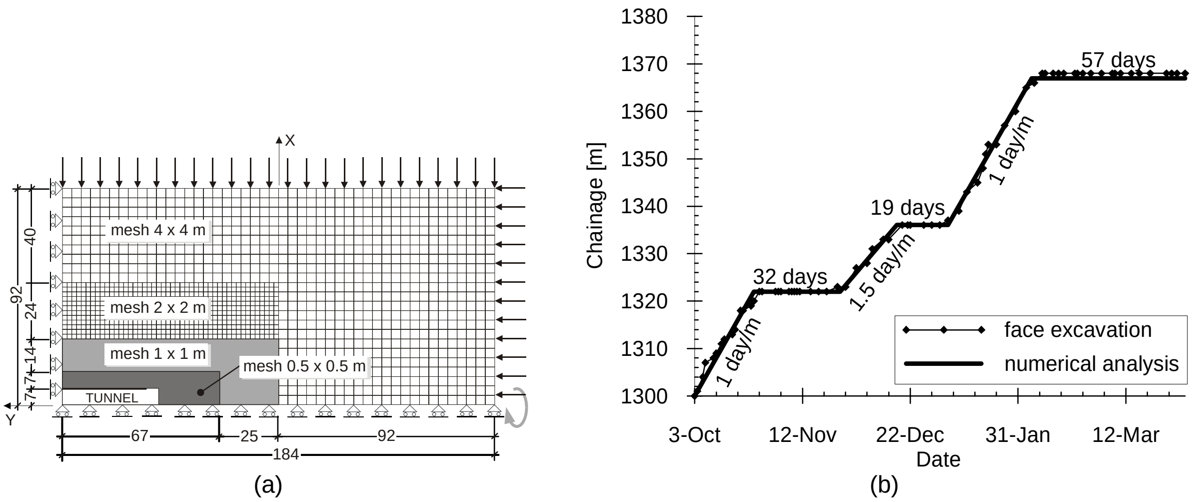

Figure 9 (a) Sketch of the finite difference grid of Saint Martin La Porte tunnel and
(b) adopted chronological sequence of excavation

The overburden is approximately 300 m and the initial vertical stress is assumed to be 8.4 MPa, with the stress ratio (K_0) equal to 1 (i.e. hydrostatic conditions). The constitutive parameter obtained by numerical back-analysis of the section at chainage 1311 m are reported in Table 4. Figure 10 shows the comparison of computed and measured values in terms of radial displacement for the section at chainage 1311 m. The agreement of the numerical results with the mean curve is excellent, notwithstanding the scattering of the monitoring data due to the heterogeneity and anisotropy of the rock mass. It is worth to notice that with the same constitutive model the radial displacements monitored in cross sections which exhibit a similar deformational response can be well represented. Also the displacements around the tunnel monitored with the multi-position borehole extensometers can be reproduced satisfactorily.

6 Conclusions

Three constitutive models (CVISC, VIPLA, SHELVIP), each one with different degrees of complexity for representing the time dependent behaviour of rock, have been discussed. Among them, of particular interest is the newly developed Stress Hardening ELastic VIscous Plastic model (SHELVIP), which is shown to describe the main features of behaviour observed during excavation of large size tunnels which exhibit severely squeezing conditions.
The SHELVIP model has been derived from the Perzyna's overstress theory, by adding a time independent plastic component. According to the classical theory of elastoplasticity, the time-independent plastic strains

develop only when the stress point reaches the plastic yield surface defined by the Drucker-Prager criterion. The viscoplastic strain rates develop only if the effective stress state exceeds a viscoplastic yield surface which is also defined by the Drucker-Prager criterion.
An innovative excavation-construction method has been described, which has been implemented in order to cope with the severely squeezing Carboniferous zone encountered in the Saint Martin access adit, along the Lyon-Turin Base Tunnel. This method utilises a two-stage excavation sequence which is based on the installation of a composite lining which incorporates a number of yielding elements formed of highly deformable concrete.
The tunnel response which is continuously monitored during face advance has been analysed. As an illustration of the application of the VIPLA model a semi-analytical solution has been used. Numerical modelling by the Finite Difference Method and the FLAC code has been applied in conjunction with the CIVISC and the SHELVIP constitutive models, with a plane strain and an axisymmetric model respectively. In all cases the computed and monitored deformations around the tunnel during face advance have been compared, showing the advantages and disadvantages of each model in describing the deformational response.

Table 4. Constitutive parameters of the SHELVIP model for Saint Martin La Porte tunnel (time in day and pressure in kPa)

E	600 MPa
ν	0.3
α_p	1.03
k_p	0.93 MPa
ω_p	0
γ	0,00008
m	2,2
n	0.18
l	0.01
α_v	0
ω_v	0.735

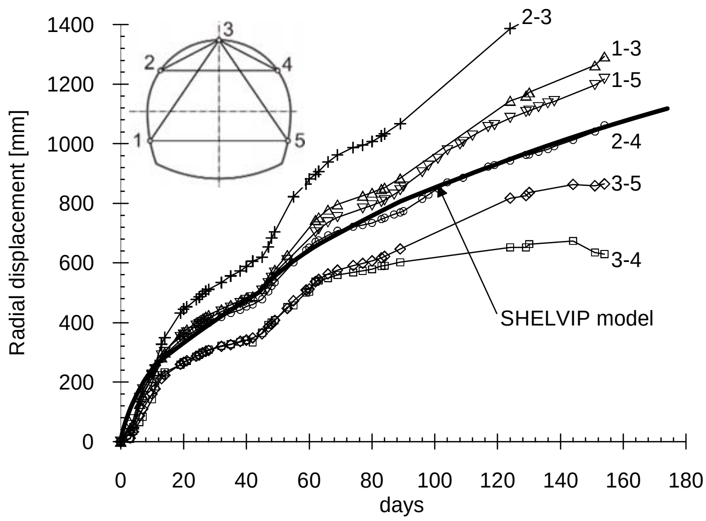

Figure 10. Computed (SHELVIP model) versus monitored convergence at chainage 1311 m model.

7 References

Barla G. 2005. Design analyses for tunnels in squeezing rock. 11th International Conference of IACMAG. Torino, June 19-24, 2005, 4, 3-22. ISBN/ISSN: 88-555-2812-2. Overview Lecture.

Barla G., Bonini M., Debernardi D. 2007. Modelling of tunnels in squeezing rock. Proceedings of the ECCOMAS Thematic Conference on Computational Methods in Tunnelling (EURO:TUN 2007), Vienna. Eberhardsteiner et al. (eds.). Vienna University of Technology, Austria, ISBN: 978-3-9501554-7-1.

Debernardi D. 2008. Viscoplastic behaviour and design of tunnels. PhD Thesis, Politecnico di Torino, Department of Structural and Geotechnical Engineering, Italy.

Itasca Inc. 2006. Flac2D 5.0, User's Manual. Minneapolis, USA.

Lemaitre J., Chaboche J.L. 1996. Mécanique des matériaux solides. Dunod, 253-341.

Nguyen-Minh, D. & Pouya, A. 1992. Une méthode d'étude des excavations souterraines en milieu viscoplastique. *Revue Française de Géotechnique* **59**, 5-14.

Panet M. 1995. Le calcul des tunnels par la méthode convergence-confinement. Presse de l'école des Ponts et chausses, Paris

Perzyna P. 1966. Fundamental Problems in Viscoplasticity. *Advances in Applied Mechanics*, Academic Press, 9, 243-377.

Sulem J., Panet M., Guenot A. 1987. Closure Analysis in Deep Tunnels. *International Journal of Rock Mechanics Mining Sciences & Geomechanics Abstracts*, **24**(3), 145-154.